J. Membrane Biol. 167, 141–149 (1999)

The Journal of
Membrane
Biology

Characteristics of Current Fluctuations Originating from Activities of Inward-Rectifier K^+ Channels in Guinea-Pig Heart Cells

Y. Yamada, N. Tohse, M. Nagashima, H. Yabu
Department of Physiology, Sapporo Medical University School of Medicine, Sapporo 060-0061, Japan

Received: 2 February 1998/Revised: 8 October 1998

Abstract. Although outward current through inward-rectifier K^+ channels has been observed in the whole-cell mode of the patch-clamp technique, no outward unitary current in single-channel studies has been recorded with the physiological ionic conditions. Hence, the relationship between single-channel activities and the inward rectification of the whole-cell current has been poorly understood. Therefore, characteristics of inward-rectifier K^+ channels in guinea-pig ventricular myocytes were assessed by the noise analysis of the K^+ current using the whole-cell patch clamp method. Partial blockade of the inward-rectifier K^+ current by Ba^{2+} was used to obtain different levels of mean current and current fluctuation as needed for variance-to-mean analysis. The plot of variance of current fluctuation against mean currents was well fitted by theoretical parabolic curves, and the unitary conductance, the open probability, and the density of functional channels were deduced. The unitary conductance of the inward-rectifier K^+ channel exhibited an inward-rectification, although the channel open probability and the density of functional channels were not much different at various holding potentials used. The unitary conductance was not changed when the intrapipette concentration of Mg^{2+} was reduced, but tended to be smaller when the pipette contained high Mg^{2+} concentration. Spermine also tended to reduce the outward unitary conductances, although the reduction was not statistically significant. These results suggest that the inward rectification in the whole-cell current was due to the inward-rectifying property of the unitary conductance of the K^+ channels. Inward rectification of the unitary conductance may be caused by blocking of the channels by both Mg^{2+} and polyamines.

Correspondence to: Y. Yamada

Key words: Inward-rectifier K^+ channel — Noise analysis — Cardiac myocytes — Polyamine — Mg^{2+} — Ba^{2+}

Introduction

Inward-rectifier K^+ current (I_{K1}) helps set the resting membrane potential and helps terminate the action potential in cardiac ventricular and atrial myocytes (Noble, 1984; Noma et al., 1984). I_{K1} is characterized by a strong inward rectification, which means that the channels conduct ions more readily in the inward direction compared to the outward direction (Hille, 1992*a*). The single channels through which I_{K1} flows have been described (Kameyama, Kiyosue & Soejima, 1983; Sakmann & Trube, 1984a; Kurachi, 1985). Although substantial outward current of I_{K1} was observed in the whole-cell patch-clamp mode (McDonald & Trautwein, 1978; Sakmann & Trube, 1984*a*), corresponding unitary outward currents were not observed in the cell-attached patch-clamp mode. On the assumption of inward rectification of the single I_{K1} channel, Sakmann and Trube (1984*a*) argued that the maximal step size of the single I_{K1} channel current expected from whole-cell records was too small to be resolved. On the other hand, Kurachi (1985) suggested that inward rectification of whole-cell current could be explained on the assumption of a linear outward unitary conductance.

Recently investigations on I_{K1} channels have revealed a steeply voltage-dependent block of the channels by intracellular polyamines (Ficker et al., 1994; Lopatin, Makhina & Nichols, 1994; Falker et al., 1995) and Mg^{2+} (Matsuda, Saigusa & Irisawa, 1987; Vandenberg, 1987) which may cause the strong inward rectification. Mg^{2+} obstructs the inner mouth of I_{K1} channels with rapid kinetics, which resulted in a flickering block of I_{K1} channels (Matsuda, 1988; Yamashita et al., 1996). Therefore,

the unitary current appears to show the inward rectification. This mechanism may be correlated with the prediction by Sakmann and Trube (1984*a*). On the other hand, polyamines obstruct the inner mouth of the channels with slower kinetics. In single-channel recordings, the channels only show open or blocked state in the outward direction. The current through open channels do not exhibit the inward rectification (Ficker et al., 1994; Yamashita et al., 1996). This mechanism corresponds with the prediction by Kurachi (1985). However, these data of Mg^{2+}- and polyamine-induced block of single I_{K1} channels were obtained in unphysiological conditions with cell-attached patch pipettes containing high K^+ solutions. It is still unknown whether single I_{K1} channels exhibit inward rectification under physiological conditions (e.g., $[K^+]_o$ = 4–6 mM).

Noise analysis is another method of analyzing characteristics of single-channel activities. To understand the relationship between the inward rectification of the whole-cell current and the single-channel activities, we estimated the single-channel characteristics of I_{K1} in isolated guinea-pig ventricular myocytes using noise analysis of the macroscopic I_{K1} in a physiological ionic condition. Variance-to-mean analysis utilizes the parabolic relationship between variance of current and mean current (Anderson & Stevens, 1973). However, this method cannot be directly applied to time-independent current like I_{K1} because different levels of mean current and current fluctuation are required to obtain a parabolic curve. Therefore, we used partial blockade of I_{K1} by external Ba^{2+}.

Material and Methods

Cell Preparation

Single ventricular myocytes were enzymatically isolated from the left ventricle of guinea-pig hearts as described previously (Tohse, 1990). In brief, the hearts were removed from guinea pigs, anaesthetized with pentobarbitone sodium. The excised heart was perfused in a Langendorff apparatus with 0.02–0.04% collagenase (Wako Pure Chemical Industries, Osaka, Japan) dissolved in a nominally Ca^{2+}-free Tyrode solution. After 30 min digestion, the left ventricle was rinsed with a Kraftbrühe (KB) solution (Isenberg & Klöckner, 1982) and cut into small pieces and shaken vigorously to separate cells. The cell suspension in the KB solution was stored in a refrigerator at 4°C for later use.

Patch Clamp Recordings

Whole-cell patch clamp recordings were made with a patch clamp amplifier (Axopatch-1D, Axon Instruments, Foster City, CA) according to the standard techniques. The patch pipettes had tip resistance of 2–4 MΩ. The cells were placed in a perfusion chamber attached to an inverted microscope (IMT-2, Olympus, Japan), and constantly superfused with external solutions (their compositions are described later) at 36 ± 1°C. Voltage stimulation and data acquisition were performed by the pCLAMP software (v.5.51, Axon Instruments) on a 486 DOS/V computer (Compaq ProLinea 466, Compaq Computer, Houston, TX) through the Labmaster TL-1 interface (Axon Instruments). When current records for the variance-to-mean studies were taken, current signals were low-pass filtered at 500 Hz (four-pole Bessel filter), sampled at 2 kHz, and stored on a hard disk. To obtain the power density spectrum, a Fast Fourier Transform (FFT) algorithm included in Microsoft Excel (Microsoft, Redmond, WA) was used. Current signals were filtered at 3 or 100 Hz by a filter with Butterworth characteristics (E-3201-A, NF Electronic Instrument, Yokohama, Japan) and sampled at 10 or 250 Hz. No leak compensation was made because only data with almost no leak were used. The data were off-line analyzed on a personal computer (Macintosh Centris 650, Apple Computer, Cupertino, CA). Cell capacitance was measured as an instantaneous change in membrane current when a ramp pulse (1 V/sec) was applied to the cell. The average capacitance was 113.4 ± 6.62 pF (n = 30). The liquid junction potential between the pipette solution and the external solution was measured to be −9 mV; therefore, all values of potentials were corrected by this value.

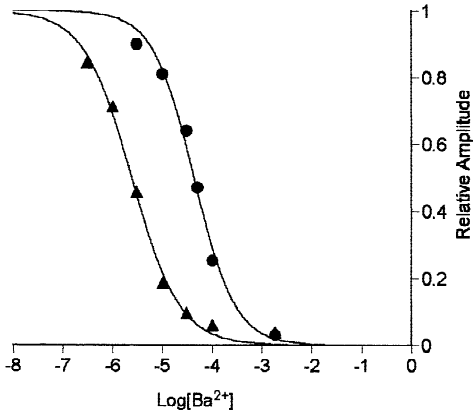

Fig. 1. Representative concentration-response relations between Ba^{2+} for partial block and the relative amplitude of I_{K1} at holding potentials (HPs) of −59 mV (● outward current) and −109 mV (▲ inward current). To determine the proper concentrations of Ba^{2+} to block I_{K1}, steady-state I_{K1} was recorded at various concentrations of Ba^{2+}. Each data point is expressed relative to I_{K1} in the absence of Ba^{2+}. The smooth curves are obtained by the least-squares fit with Eq. 1. Dissociation constants at HPs of −59 and −109 mV were 43.6 and 2.44 μM, respectively. Ba^{2+}-induced block of I_{K1} was voltage dependent. Hill coefficients were 1.06 (−59 mV) and 0.91 (−109 mV) indicating 1:1 binding.

Data Analysis

All fitting procedures were done with DeltaGraph Pro ver 3.0.4 (Delta Point, Monterey, CA) using the least-squares method. We used Ba^{2+} to obtain different levels of mean I_{K1}, necessary to employ variance-to-mean analysis. Figure 1 shows representative concentration-response relations of Ba^{2+} for I_{K1}. As Ba^{2+} at concentrations of 0.3 μM–1.8 mM allowed the minimal to the maximal change in mean I_{K1} both at −59 and −109 mV, we used these concentrations of Ba^{2+} for variance-to-mean analysis. Data for concentration-response relation were fitted to Eq. 1.

$$\frac{I}{I_{MAX}} = \frac{1}{1 + ([Ba^{2+}]/K_d)^{n_h}} \quad (1)$$

where I is the Ba^{2+} blocked current, I_{MAX} is the steady-state current in the absence of Ba^{2+}, $[Ba^{2+}]$ is a concentration of Ba^{2+} in the external solution, K_d is the dissociation constant, n_h is the Hill-coefficient.

To obtain time constants from current relaxations caused by Ba^{2+}-block or -unblock of I_{K1}, Eq. 2 was used:

$$I_{(t)} = I_{ss} - I_v \cdot \exp\left(-\frac{t}{\tau}\right) \quad (2)$$

where $I_{(t)}$ is the time-dependent current, I_{ss} is the steady-state current, I_v is an adjustable constant, τ is the time constant.

All values are presented in terms of mean ± SEM. Differences between two groups were evaluated by Student's t test where appropriate. One-way ANOVA or two-way ANOVA was first carried out to test for any differences among the mean values of multiple subgroups. When a significant F value was obtained by two-way ANOVA, intergroup comparisons were performed by Fisher's protected least significant difference (Fisher's PLSD) if an interaction was not significant. When an interaction was significant, one-way ANOVA followed by Fisher's PLSD was performed on the same data for pairwise comparisons. Significance was established at P values < 0.05.

Experimental Solutions

The composition of Tyrode solution was (in mM): NaCl 143, KCl 5.4, $CaCl_2$ 1.8, $MgCl_2$ 0.5, NaH_2PO_4 0.33, Glucose 5.5, and HEPES 5 (pH = 7.4, titrated by 1 N NaOH). The KB solution was composed of (in mM): KCl 40, KOH 70, KH_2PO_4 20, *l*-glutamic acid 50, taurine 20, $MgCl_2$ 3, EGTA 1, glucose 10, and HEPES 10 (pH = 7.4, titrated by 1 N KOH). The external solution for whole-cell recordings contained (in mM): choline-Cl 143, KCl 5.4, $CoCl_2$ 1.8 mM, $MgCl_2$ 0.5, glucose 5.5, HEPES 5 (pH = 7.4, titrated by 1 N NaOH), and various concentrations of $BaCl_2$ (0.3 μM–1.8 mM). For solutions containing various concentrations of Ba^{2+}, Ba^{2+} was simply added to the external solution, except when 1.8 mM $BaCl_2$ was used, $CoCl_2$ was omitted. KCl was omitted from the external solution to make the K^+-free solution.

The composition of the pipette solution for whole-cell recordings was (in mM): *l*-glutamic acid 110, KCl 20, KOH 110, $MgCl_2$ 3 Na_2ATP 5, creatine phosphate 5, EGTA 10, and HEPES 5 (pH = 7.4, titrated by 1N KOH). The estimated concentration of free Mg^{2+} was 16 μM by the formula developed by Fabiato and Fabiato (1979). To prepare the pipette solution containing 1.6 mM free Mg^{2+}, a total of 8 mM $MgCl_2$ was added. For the Mg^{2+}-free solution, 10 mM EDTA was added in place of 5 mM EGTA, the concentration of free Mg^{2+} was estimated to be less than 10^{-8} M. Spermine at 50 or 500 μM was added to the Mg^{2+}-free pipette solution.

Results

Current Fluctuations of Steady-State I_{K1} in the Presence of Ba^{2+}

To determine whether current fluctuation in our experimental condition was derived mainly from block and unblock of I_{K1} channels by Ba^{2+}, we compared results from two different methods to analyze blocking kinetics. One method utilizes voltage-dependence of Ba^{2+} block of I_{K1} channels. Because of this voltage dependency, a current relaxation is observed when a step command pulse of voltage is applied to a cell in an external solution containing Ba^{2+}. A time constant is calculated from this decay (the current relaxation experiment). The other method is a steady-state noise analysis (Anderson & Stevens, 1973).

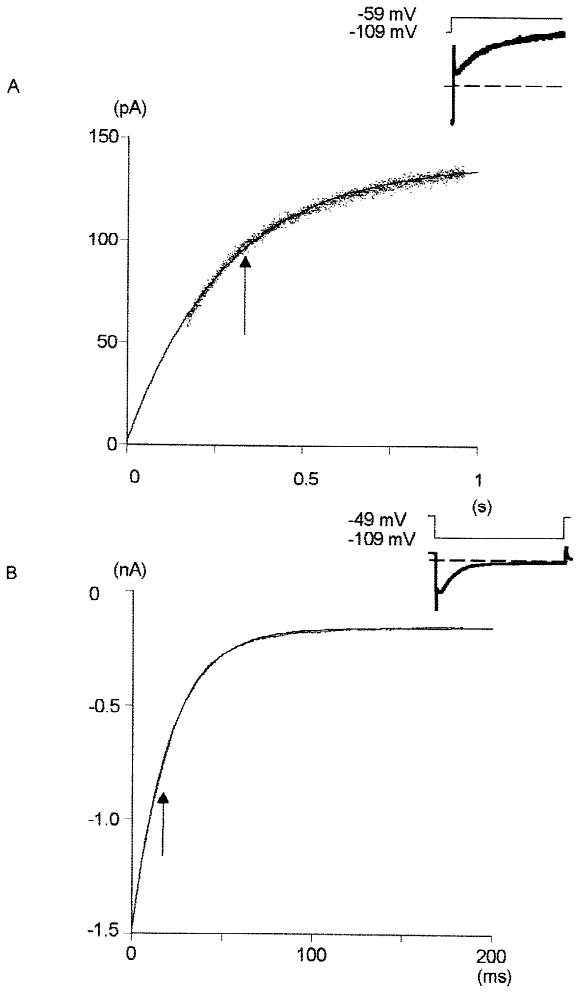

Fig. 2. Time-dependent changes of I_{K1} due to Ba^{2+}-induced block and unblock. Dots indicate time courses of unblocking (*A*) and blocking (*B*) of I_{K1} by Ba^{2+}. Actual current tracings are shown in the inset. Solid lines were obtained by the least squares fit with Eq. 2 (*see* text for details). Arrows indicate the time constants derived from Eq. 2, and these are 286 msec in panel *A* and 22.4 msec in panel *B*. Inset: Currents recorded during a 1-sec pulse to −59 mV from a HP of −109 mV (*A*) and during a 200 msec pulse to −109 mV from a HP of −49 mV (*B*); the external solution contained 0.1 mM Ba^{2+} to partially block the channel. The horizontal dashed line shows the zero current level. Data were low-pass filtered at 2 kHz (four-pole Bessel type) and sampled at 500 Hz.

Figure 2*A* shows a representative current relaxation experiment in the presence of 0.1 mM Ba^{2+}. When the membrane was depolarized from −109 to −59 mV, the outward current of I_{K1} increased gradually (*see* inset) because Ba^{2+} blocked I_{K1} more potently at −109 than at −59 mV. The time-dependent increment of the outward

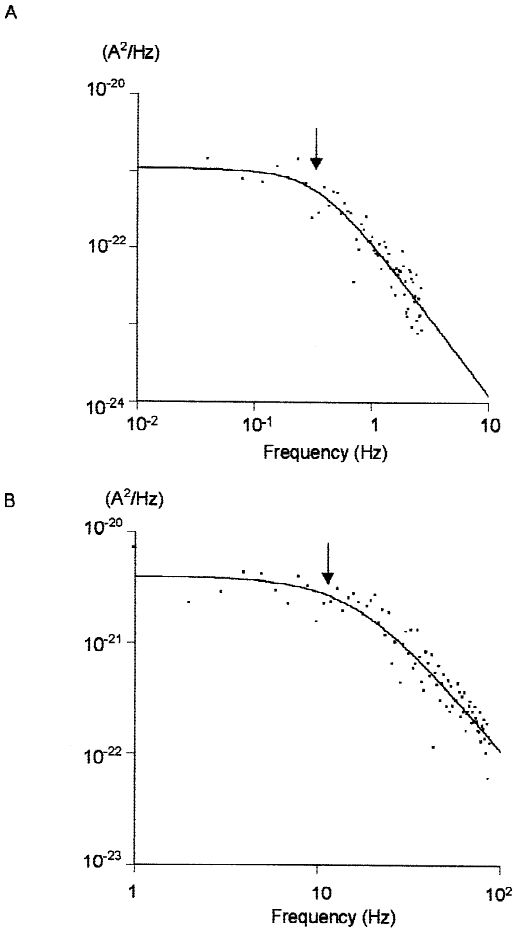

Fig. 3. Power density spectra of Ba^{2+}-blocked I_{K1} at HPs of −59 (*A*) and −109 mV (*B*). Digitized fluctuations were transformed into the frequency domain with the FFT algorithm. Each spectrum consists of mean values from 10 different recordings. The background noise in K^+-free solution was subtracted. Dots are calculated power density spectra. Solid lines were obtained by the least-squares fit with Eq. 3 (*see* text for details). Arrows indicate the location of the corner frequencies, and these values are 0.342 Hz in panel *A* and 15.2 Hz in panel *B*. Data were low-pass filtered at 3 Hz (*A*) or 100 Hz (*B*) with the Butterworth characteristics and sampled at 10 Hz (*A*) and 250 Hz (*B*).

current may be produced by the release of Ba^{2+} from the I_{K1} channels. A single-exponential function fitted well the time course of the increment. This finding is consistent with the first-order kinetics of block of I_{K1} channels by Ba^{2+}. The time constant obtained at −59 mV was 286 msec.

In Fig. 2*B*, the time constant of block of inward I_{K1} by Ba^{2+} was determined. Ba^{2+} gradually reduced the inward current because of plugging the pores of I_{K1} channels. The current decay was also fitted well by a single exponential. The time constant of block by Ba^{2+} was 22.4 msec.

Figure 3 shows the power density spectra of the current fluctuations obtained in external solution containing 0.1 mM Ba^{2+}. The outward current at a holding potential (HP) of −59 mV (Fig. 3*A*) and the inward current at −109 mV (Fig. 3*B*) were obtained from the same cells shown in Fig. 2. The fluctuations may originate from I_{K1} because external K^+-free solution abolished fluctuations (*data not shown*). It has been reported that the absence of external K^+ closes the I_{K1} channels (Hall, Hutter & Noble, 1962; Tohse, Kameyama & Irisawa, 1987). The current fluctuations were transformed with FFT to yield the power density spectra (dots in Fig. 3).

A model that Ba^{2+} blocks each I_{K1} channel by first-order kinetics independently should give a spectral distribution of energy density according to Eq. 3 (Anderson & Stevens, 1973):

$$S_{(f)} = \frac{S_{(0)}}{1 + (f/f_c)^2} \tag{3}$$

where $S_{(f)}$ = the power density, $S_{(0)}$ = the power density at frequency $f = 0$, and f_c = the corner frequency. According to the previous report (Anderson & Stevens, 1973) this power distribution is Lorentzian, and the corner frequency is related to the relaxation time constant (τ) by

$$\tau = \frac{1}{2\pi \cdot f_c} \tag{4}$$

The solid lines were Lorentzian curves fitted to the power density spectra. The corner frequencies were derived from these curves, and the time constants calculated were 465 msec and 10.5 msec, respectively. These values were comparable to those obtained from the current relaxation experiments in Fig. 2. Time constants obtained by the current relaxation experiments and the steady-state noise analysis were not significantly different by unpaired *t*-test (327.7 ± 31.4 and 450.8 ± 66 at −59 mV ($n = 4$), 16.1 ± 3.7 and 9.3 ± 0.6 at 109 mV ($n = 3$)). The compatible time constants derived from two different methods support the idea that Ba^{2+}-induced block and unblock of I_{K1} channels caused fluctuations of steady-state K^+ currents.

The Variance-to-Mean Analysis of Ba^{2+}-induced Current Fluctuations of I_{K1}

We used various concentrations of Ba^{2+} to obtain different levels of steady-state I_{K1}. Inset of Fig. 4*A* shows representative fluctuations of I_{K1} at a HP of −59 mV. The amplitude of the current fluctuation recorded with 0.1 mM Ba^{2+} obviously increased, compared to that without Ba^{2+}. On the other hand, the amplitude of the current fluctuation obtained with 1.8 mM Ba^{2+} was smaller than that with 0.1 mM. The same tendency was observed at a HP of −109 mV (*see* inset of Fig. 4*B*). Because Eq. 5

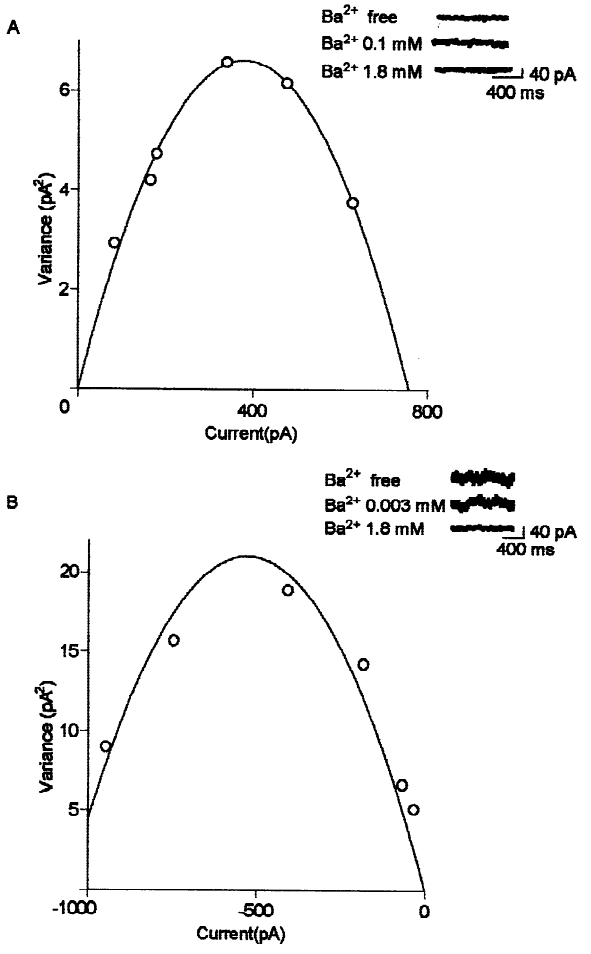

Fig. 4. Variance-to-mean analysis of I_{K1} at a HPs of −59 mV (*A*) and −109 mV (*B*) in the presence of Ba^{2+}. The variance and the mean current were averaged over 5 different traces, and the variance was plotted as a function of the mean current. As the background variance computed from currents in the K^+-free solution was markedly small, compared with the variance in the presence of Ba^{2+}, they were not subtracted. Solid curves were obtained by fitting Eq. 5 to the data (○) (*see* text for details). Insets: Fluctuations of steady-state I_{K1} were recorded in the presence of various concentrations of Ba^{2+} at a holding potential of −59 mV (*A*) or −109 mV (*B*).

holds for the relationship between variance and mean current (Noma, Peper & Trautwein, 1979), the data were fitted by the least-squares method with Eq. 5.

$$\sigma^2 = i \cdot I - \frac{I^2}{N} \tag{5}$$

where σ^2 = the variance, i = the unitary current, I = the mean current, N = the number of channels per cell. The data displayed in Fig. 4 were best fitted with Eq. 5 using parameters (i = 0.035 pA, N = 21637 for −59 mV, i = −0.066 pA, N = 18467 for −109 mV).

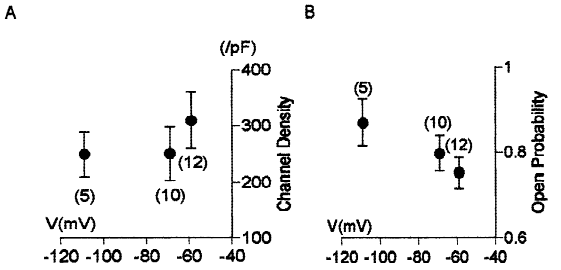

Fig. 5. Densities of channels (*A*) and the channel open probabilities (*B*) were plotted against membrane potentials. Densities of channels were obtained by dividing the number of channels per cell by the total cell capacitance. Data are shown as mean ± SEM. Numbers in parentheses indicate the number of cells examined. No significant difference was detected by one-way ANOVA. The intrapipette Mg^{2+} concentration was 16 μM.

Inward Rectification Property of the Unitary Conductances

Figure 5*A* shows the summary of the densities of channels plotted against membrane potentials with data from different cells. The calculated densities exhibited no voltage-dependency. Figure 5*B* shows the voltage dependence of the channel open probability. The channel open probability (P) was calculated using Eq. 6:

$$P = \frac{I}{N \cdot i} \tag{6}$$

where P = the channel open probability, i = the unitary current, $I = I_{K1}$ in the absence of Ba^{2+}, N = the number of channels per cell. The open probabilities tended to be higher when the current flowed inwardly than outwardly. This tendency might explain the inward rectification. However, no statistically significant difference was seen among values at various HPs.

Figure 6 shows the relationship between the unitary conductances and holding potentials that was obtained from summarized data of different cells. The unitary current in the outward direction was smaller than expected from that in the inward direction if the conductance of open channel is ohmic. The unitary conductance in itself exhibited an inward rectifying property, perhaps responsible for inward rectification observed in the whole-cell mode.

The Role of Internal Mg^{2+} in Inward Rectification of The Unitary Conductance

It has been proposed that inward rectification is due to block of channels by internal polyamines (Ficker et al., 1994; Lopatin et al., 1994; Falker et al., 1995) and Mg^{2+} (Matsuda et al., 1987; Vandenberg, 1987). If so, our results imply that internal polyamines and Mg^{2+} reduce

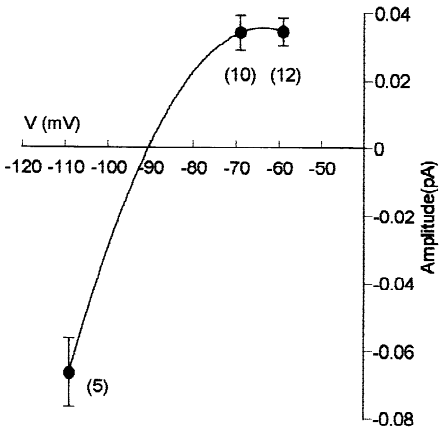

Fig. 6. Current/voltage relationship for the unitary conductance. Data are shown as mean ± SEM. Numbers in parentheses indicate the number of cells examined. The solid curve was obtained by fitting the polynomial function to the data. Note the inward rectification property. The intrapipette Mg^{2+} concentration was 16 μM.

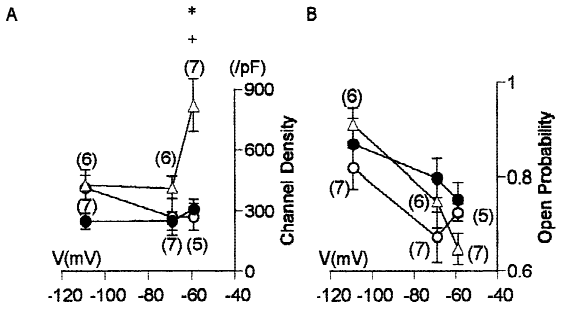

Fig. 7. (*A*) Voltage dependency of density of channel is shown at three different internal Mg^{2+} concentrations: Mg^{2+} free (○); 16 μM (●); 1.6 mM Mg^{2+} (△). Two-way ANOVA detected significant difference among subgroups. Differences were significant by Fisher's PLSD between Mg^{2+} free and 1.6 mM Mg^{2+} (+$P < 0.05$) and between 16 μM Mg^{2+} and 1.6 mM Mg^{2+} (*$P < 0.05$). (*B*) Voltage dependency of the channel open probabilities is shown for the same Mg^{2+} concentrations as in panel *A*. No significant difference was seen among these groups by two-way ANOVA. The data for 16 μM Mg^{2+} are the same as those shown in Fig. 5.

Table 1. Comparison of data for various intra-pipette concentrations of Mg^{2+}

	$[Mg^{2+}]$			
	0	16 μM	1.6 mM	*P*-value
A. HP = −59 mV				
Unit conductance (pS)	1.1 ± 0.27	1.1 ± 0.14	0.5 ± 0.05	$p < 0.05$
Open probability	0.725 ± 0.018	0.752 ± 0.036	0.647 ± 0.032	NS
Channel density (/pF)	271 ± 67.6	310 ± 50.3	823 ± 130.2	$P < 0.05$
B. HP = −109 mV				
Unit conductance (pS)	3.2 ± 0.5	3.4 ± 0.5	2.5 ± 0.23	NS
Open probability	0.819 ± 0.044	0.87 ± 0.055	0.912 ± 0.036	NS
Channel density (/pF)	417 ± 57.8	249 ± 39.5	430 ± 69.5	NS

Unit conductance were computed by dividing the unit amplitudes by the driving forces that were calculated as HPs minus E_K (−89 mV). Values of open probabilities and channel densities were the same as those in Fig. 7. Values are mean ± SEM. *P* values were obtained by Fisher's PLSD.

the unitary conductance in the outward direction. To ascertain the effect of intracellular Mg^{2+} on the unitary conductance of I_{K1}, we compared results obtained with the pipettes containing Mg^{2+} at concentrations of 1.6 mM, 16 μM, and Mg^{2+}-free (10 mM EDTA). When we used pipettes containing 16 μM Mg^{2+} and Mg^{2+}-free, the channel densities were almost identical. However, the channel density was increased using pipettes containing 1.6 mM Mg^{2+} (Fig. 7*A*, Table 1). This change is not expected by Mg^{2+}-blocking of outward I_{K1}. Figure 7*B* shows the channel open probability plotted against membrane potential. Open probabilities were significantly higher in the inward than in the outward direction. However, there was no significant difference among 1.6 mM Mg^{2+}, 16 μM Mg^{2+} and Mg^{2+}-free (*also see* Table 1).

Figure 8 shows the effect of internal Mg^{2+} on the unitary conductance. In experiments using 1.6 mM Mg^{2+}, the unitary conductance in the outward direction was smaller than in those with 16 μM Mg^{2+}. However, no change was observed when we used Mg^{2+}-free. These data suggest that internal Mg^{2+} contributes to the reduction of the unitary conductance in the outward direction, but cannot entirely explain the inward rectification property of single-channel I_{K1}.

The Role of Internal Polyamines in Inward Rectification of the Unitary Conductance

The results with Mg^{2+} suggest that internal polyamines may also play some role in reducing the unitary conductance in the outward direction. To determine whether polyamines cause the reduced unitary conductance, spermine at 50 or 500 μM was added to the Mg^{2+}-free

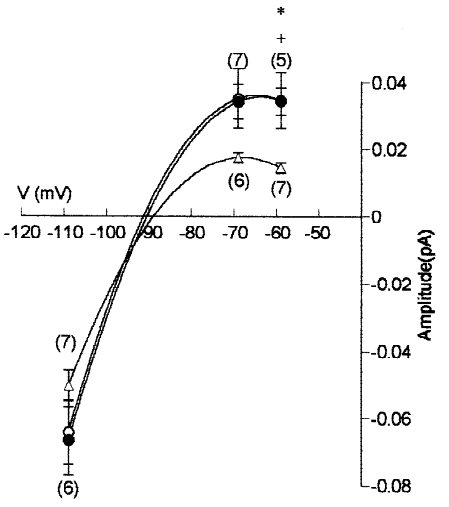

Fig. 8. The effect of internal Mg^{2+} on the current/voltage relationship for the unitary conductance. ○, ● and △ represent Mg^{2+}-free, 16 μM Mg^{2+}, and 1.6 mM Mg^{2+}, respectively. Voltage dependency of the unitary conductance was significantly different among subgroups by two-way ANOVA. Differences were statistically significant between Mg^{2+}-free and 1.6 mM Mg^{2+} (+$P < 0.05$) and between 16 μM Mg^{2+} and 1.6 mM Mg^{2+} (*$P < 0.05$) by Fisher's PLSD. The data of 16 μM Mg^{2+} are the same as those shown in Fig. 6.

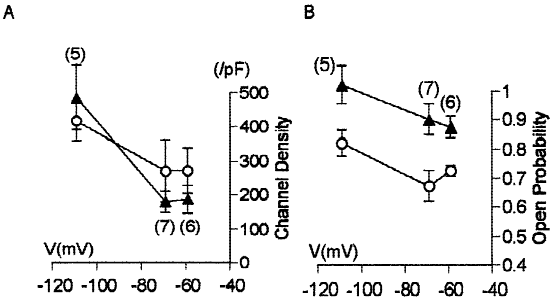

Fig. 9. Voltage dependencies of density of channels (*A*) and the channel open probability (*B*) calculated from the experiments when the pipettes contained 50 μM spermine (▲) or not (○). Two-way ANOVA did not detect significant difference between the two groups in panel *A* but did in panel *B*. The control data without spermine are the same as those shown in Fig. 7.

internal solution. We chose spermine because a physiological concentration of free spermine was shown to have strong effects on a cloned inward rectifier K^+ channels, while spermidine was reported to be 100-fold less effective than spermine, and putrescine was 10-fold less abundant and 10,000-fold less effective than spermine (Bianchi et al., 1996; Falker et al., 1995). When we used 500 μM spermine, I_{K1} recorded in the whole-cell mode decreased gradually in both the inward and outward directions throughout the voltage range tested (*data not shown*). Because only small amounts of outward currents could be observed after intracellular perfusion with

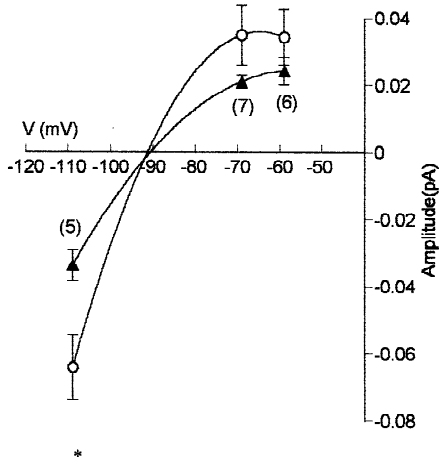

Fig. 10. Effect of internal spermine on the current/voltage relationship for the unitary conductance. Data represent the averaged values from the experiments when the pipettes included 50 μM spermine (▲) or no spermine (○). There was significant difference between the two groups by two-way ANOVA. Difference was also significant by Fisher's PLSD (*$P < 0.05$). The data without spermine are the same those as shown in Fig. 8.

500 μM spermine, spermine was reduced to 50 μM for the noise analysis. Figure 9 shows the effects of internal application of 50 μM spermine on density of channels and the channel open probability (*also see* Table 2). Although channel density tended to be reduced in the outward direction, it was not significant. Paradoxically, the channel open probabilities were increased by spermine at all HPs examined. The unitary conductance in the outward direction also tended to be reduced with 50 μM spermine, but it was not significant. In contrast, spermine significantly reduced the unitary conductance in the inward direction, and may account for the reduced inward I_{K1} produced by 500 μM spermine (Fig. 10, Table 2).

Discussion

As mentioned in the Introduction section, different levels of mean current and current noise are needed for variance-to-mean analysis. Therefore, we prepared the external solutions containing various concentrations of Ba^{2+}. This method assumes that current fluctuations are due to Ba^{2+} block and unblock of I_{K1} channels and not to change in the unitary conductance. We checked the former assumption by comparing the time constants derived from steady-state I_{K1} with those obtained by current relaxation experiments. The similar time constants obtained by these two methods supports the first assumption. Although we could not verify the latter assumption, it does not seem unreasonable because it was reported that the unitary conductance of I_{K1} channels was the same in the presence or absence of external Ba^{2+} (Kameyama et al., 1983; Sakmann & Trube, 1984*b*).

Table 2. Comparison of data with and without intra-pipette spermine

	[Spermine]		
	0	50 μM	*P*-value
A. HP = −59 mV			
Unit conductance (pS)	1.1 ± 0.27	0.8 ± 0.14	NS
Open probability	0.725 ± 0.018	0.874 ± 0.037	+p < 0.05
Channel density (/pF)	271 ± 67.6	187 ± 41.1	NS
B. HP = −109 mV			
Unit conductance (pS)	3.2 ± 0.5	1.7 ± 0.23	+p < 0.05
Open probability	0.819 ± 0.044	1.02 ± 0.06	*p < 0.05
Channel density (/pF)	417 ± 57.8	486 ± 94.3	NS

Unit conductance were computed in the same way as in Table 1. Values of open probabilities and channel densities were the same as those in Fig. 9. Values are mean ± SEM. *P* values were obtained by two-way ANOVA (*) and by Fisher's PLSD (+).

In this study, the inward rectification property of the unitary conductance might mainly explain the inward rectification observed in the whole-cell mode. Under the present experimental condition, the calculated equilibrium potential for K^+ was −89 mV. Therefore, the estimated chord conductance in the inward direction was 2.5–3.4 pS, which is not far from the value expected from previous reports (Kameyama et al., 1983; Sakmann & Trube, 1984a; Kurachi, 1985). However, the outward conductance (0.5–1.1 pS) was smaller than the inward one (Table 1). The channel open probabilities tended to be higher at the hyperpolarized potential than at depolarized potentials. However, statistically significant differences were not always seen. Thus, the voltage dependence of the channel open probability may contribute little to the inward rectification of I_{K1} seen in the whole-cell mode. In some experiments, the channel densities at the depolarized potentials were higher than at the hyperpolarized potentials. However, this observation cannot explain the inward rectification property of I_{K1} in the whole-cell mode, because the increased number of channels at depolarized potentials should increase outward current, and not decrease it.

The reduced outward unitary conductance does not necessarily mean real decrease in the maximum rate of passing K^+ ions through this channel. If kinetics of block and/or unblock is faster than the limit of our time resolution, individual openings become blurred and are seen only as extra ''noise'' and a lowered conductance (Hille, 1992*b*). The reduced unitary outward current of K_{ATP} channels in the presence of internal Mg^{2+} (Horie, Irisawa & Noma, 1987) is a good example of the blurred opening.

Intracellular Mg^{2+} and polyamines cause inward rectification (Ficker et al., 1994; Falker et al., 1995; Lopatin, Makhina & Nichols, 1995; Ishihara, Hiraoka & Ochi, 1996). Therefore, it is highly probable that the outward unitary conductance is reduced by very fast block of I_{K1} by Mg^{2+} and/or polyamines. To check this possibility, we prepared pipettes which contained Mg^{2+} at a higher concentration (1.6 mM free Mg^{2+}) and almost no Mg^{2+}. As kinetics of Mg^{2+} block and unblock of I_{K1} is believed to be fast (Ishihara et al., 1989), we speculated that the reduced outward unitary conductance is due to the fast block by Mg^{2+}. When the intrapipette concentration of Mg^{2+} was increased to 1.6 mM, the inward rectification property became stronger. On the other hand, the inward rectification property was still observed when we used pipettes with no Mg^{2+} (*see* Fig. 8 and Table 1). These data indicate that the internal Mg^{2+} reduces the outward unitary conductance, but is not entirely responsible for the inward rectification property.

Results with changes in the internal Mg^{2+} concentration suggest that polyamines and/or intrinsic gatings may play roles to reduce the outward unitary conductance. Spermidine and putrescine are reported to have fast enough kinetics. Ishihara et al. (1997) observed an instantaneous activation on hyperpolarization in almost a Mg^{2+}-free environment, and attributed this to a rapid relief of endogenous spermidine block. Ficker et al. (1994) showed that putrescine reduced the unitary conductance in the outward direction in single-channel studies on mutant IRK1 channels. However, as stated in Results, we thought spermidine and putrescine was not effective and/or abundant enough to play some roles in reducing the outward unitary current on physiological environment. Although the blocking kinetics of spermine is generally thought to be slow (Ishihara et al., 1997; Yamashita et al., 1997), there is the report that indicates spermine has fast enough kinetics to cause the inward rectification. Lopatin et al. (1995) proposed a very fast kinetic block by spermine itself for the HRK1 channel expressed in *Xenopus* oocytes. If spermine causes the inward rectification of the unitary conductance, an increment in concentration of intracellular spermine must reduce the outward unitary conductance further. Our data

showed that spermine had a tendency to induce stronger inward rectification, but no statistical significance was seen (*see* Fig. 10 and Table 2). Recently Shyng et al. (1996) reported that decreasing the level of putrescine doubled macroscopic potassium conductance through a cloned I_{K1} channel in one of Chinese hamster ovary cell line, as assessed by ^{86}Rb flux assay. Therefore, the endogenous spermidine and/or putrescine may play more important roles than spermine in reducing the unitary conductance. Another possibility is that intrinsic gatings of the channel cause the inward rectification.

In the present study, high intracellular Mg^{2+} increased the density of functional channels. On the other hand, spermine tended to decrease the densities of functional channels (*see* Figs. 7, 9, Table 1 and 2). This phenomenon can be explained by a difference of blocking kinetics between Mg^{2+} and polyamines. In the presence of Mg^{2+}, I_{K1} channel may quickly transit between an open state and a short-lived blocked state. Therefore, the Mg^{2+}-blocked I_{K1} channel seems to be functional with a reduced unitary conductance, because the channel cannot transit to long-lasting closed state (shut without Mg^{2+}). On the other hand, I_{K1} channel closes and hardly transits to the open state in the presence of polyamines. Hence, I_{K1}-channel slowly blocked by polyamines appears to be as nonfunctional channel.

The authors thank Prof. Nicholas Sperelakis, University of Cincinnati College of Medicine, for his advice and discussion on the manuscript.

References

Anderson, C.R., Stevens, C.F. 1973. Voltage clamp analysis of acetylcholine produced endplate current fluctuations at frog neuromuscular junction. *J. Physiol.* **235:**655–691

Bianchi, L., Roy, M.L., Taglialatela, M., Lundgren, D.W., Brown, A.M., Ficker, E. 1996. Regulation by Spermine of Native Inward Rectifier K^+ Channels in RBL-1 Cells. *J. Biol. Chem.* **271:**6114–6121

Fabiato, A., Fabiato, F. 1979. Calculator programs for computing the composition of the solutions containing multiple metals and ligands used for experiments in skinned muscle cells. *J. Physiol.* **75:**463–505

Falker, B., Brandle, U., Glowatzki, E., Weidemann, S., Zenner, H.-P., Ruppersberg, J.P. 1995. Strong voltage-dependent inward rectification of inward rectifier K^+ channels is caused by intracellular spermine. *Cell* **80:**149–154

Ficker, E., Taglialatela, M., Wible, B.A., Henley, C.M., Brown, A.M. 1994. Spermine and Spermidine as gating molecules for inward rectifier K^+ channels. *Science* **266:**1068–1072

Hall, A.E., Hutter, O.F., Noble, D. 1962. Current-voltage relations of purkinje fibres in sodium-deficient solutions. *J. Physiol.* **166:**225–240

Hille, B. 1992*a*. Potassium channels and chloride channels. *In:* Ionic Channels of Excitable Membranes. 2nd ed. pp. 115–139. Sinauer Associates, Sunderland

Hille, B. 1992*b*. Mechanisms of block. *In:* Ionic Channels of Excitable Membranes. 2nd ed. pp. 390–422. Sinauer Associates, Sunderland

Horie, M., Irisawa, H., Noma, A. 1987. Voltage-dependent magnesium block of adenosine-triphosphate-sensitive potassium channel in guinea-pig ventricular cells. *J. Physiol.* **387:**251–272

Isenberg, G., Klöckner, U. 1982. Calcium tolerant ventricular myocytes prepared by preincubation in a ''KB medium''. *Pfluegers Arch.* **395:**6–18

Ishihara, K. 1997. Time-dependent outward currents through the inward rectifier potassium channel IRK1: The role of weak blocking molecules. *J. Gen. Physiol.* **109:**229–243

Ishihara, K., Hiraoka, M., Ochi, R. 1996. The tetravalent organic cation spermine causes the gating of the IRK1 channel expressed in murine fibroblast cells. *J. Physiol.* **491:**367–381

Ishihara, K., Mitsuie, T., Noma, A., Takano, M. 1989. The Mg^{2+} block and intrinsic gating underlying inward rectification of the K^+ current in guinea-pig cardiac myocytes. *J. Physiol.* **419:**297–320

Kameyama, M., Kiyosue, K., Soejima, M. 1983. Single channel analysis of the inward rectifier K current in the rabbit ventricular cells. *Jpn. J. Physiol.* **33:**1039–1056

Kurachi, Y. 1985. Voltage-dependent activation of the inward-rectifier potassium channel in the ventricular cell membrane of guinea-pig heart. *J. Physiol.* **366:**365–385

Lopatin, A.N., Makhina, E.N., Nichols, C.G. 1994. Potassium channel block by cytoplasmic polyamines as the mechanism of intrinsic rectification. *Nature* **372:**366–369

Lopatin, A.N., Makhina, E.N., Nichols, C.G. 1995. The mechanism of inward rectification of potassium channels: ''Long-pore plugging'' by cytoplasmic polyamines. *J. Gen. Physiol.* **106:**923–955

Matsuda, H. 1988. Open-state substructure of inwardly rectifying potassium channels revealed by magnesium block in guinea-pig heart cells. *J. Physiol.* **397:**237–258

Matsuda, H., Saigusa, A., Irisawa, H. 1987. Ohmic conductance through the inwardly rectifying K channel and blocking by internal Mg^{2+}. *Nature* **325:**156–159

McDonald, T.F., Trautwein, W. 1978. The potassium current underlying delayed rectification in cat ventricular muscle. *J. Physiol.* **274:**217–246

Noble, D. 1984. The surprising heart: a review of recent progress in cardiac electrophysiology. *J. Physiol.* **353:**1–50

Noma, A., Nakayama, T., Kurachi, Y., Irisawa, H. 1984. Resting K conductance in pacemaker and non-pacemaker heart cells of the rabbit. *Jpn. J. Physiol.* **34:**245–254

Noma, A., Peper, K., Trautwein, W. 1979. Acetylcholine-induced potassium current fluctuations in the rabbit sino-atrial node. *Pfluegers Arch.* **381:**255–262

Sakmann, B., Trube, G. 1984*a*. Conductance properties of single inwardly rectifying potassium channels in ventricular cells from guinea pig heart. *J. Physiol.* **347:**641–657

Sakmann, B., Trube, G. 1984*b*. Voltage-dependent inactivation of inward-rectifying single-channel currents in the guinea-pig heart cell membrane. *J. Physiol.* **347:**659–683

Shyng, S.-L., Sha, Q., Ferrigni, T., Lopatin, A.N., Nichols, C.G. 1996. Depletion of intracellular polyamines relieves inward rectification of potassium channels. *Proc. Natl. Acad. Sci. USA* **93:**12014–12019

Tohse, N. 1990. Calcium-sensitive delayed rectifier potassium current in guinea pig ventricular cells. *Am. J. Physiol.* **258:**H1200–H1207

Tohse, N., Kameyama, M., Irisawa, H. 1987. Intracellular Ca^{2+} and protein kinase C modulate K^+ current in guinea pig ventricular cells. *Am. J. Physiol.* **253:**H1321–H1324

Vandenberg, C.A. 1987. Inward rectification of a potassium channel in cardiac ventricular cells depends on internal magnesium ions. *Proc. Natl. Acad. Sci. USA* **84:**2560–2564

Yamashita, T., Horio, Y., Yamada, M., Takahashi, N., Kondo, C., Kurachi, Y. 1996. Competition between Mg^{2+} and spermine for a cloned IRK2 channel expressed in a human cell line. *J. Physiol.* **493:**143–156